

# Direct numerical simulations of a double-diffusive interface in the diffusive regime

J.R. Carpenter,<sup>(1)</sup> T. Sommer<sup>(1,2)</sup> & A. Wüest<sup>(1,2)</sup>

<sup>(1)</sup>Surface Waters - Research and Management,  
EAWAG, Swiss Federal Institute of Aquatic Science and Technology;  
CH-6047 Kastanienbaum, Switzerland  
jeffcarp@gmail.com

<sup>(2)</sup>Institute of Biogeochemistry and Pollutant Dynamics,  
Environmental Sciences, ETH;  
CH-8092 Zürich, Switzerland

## Abstract

The ‘diffusive interface’, separating homogeneous regions of cold fresh water above and warm salty water below, is studied using direct numerical simulations (DNS). The simulations are designed to replicate as closely as possible conditions present in the thermohaline staircase of Lake Kivu, as well as previous laboratory experiments. The results reveal that a ‘double boundary layer’ structure is present in which the temperature interface is thicker than the salinity interface by a factor of two. This boundary layer is found to supply the mixed layers above and below the interface with buoyancy through the formation of plumes and large scale convection rolls. We also examine the applicability of the 4/3 flux law in describing the heat flux across the interface, and compare with a previous theory.

## 1 Introduction

Double-diffusive convection occurs when the water column is stratified by two opposing scalar gradients that contribute to fluid density and have different molecular diffusivities. It is found over vast regions of the world oceans (You, 2002; Kelley et al., 2003), which are both temperature ( $T$ ) and salinity ( $S$ ) stratified. Although double-diffusive (DD) convection is generally studied with temperature and salinity in mind, we shall describe results in which  $T$  simply refers to the faster diffusing component and  $S$  to the slower diffusing component, where both are expressed in density units. Two cases exist depending on whether  $T$  or  $S$  is gravitationally unstable: (i) the salt-finger case with an unstable  $S$  gradient, and (ii) the diffusive case where  $T$  is gravitationally unstable. We shall describe only the diffusive case (ii).

Observations of the  $TS$ -structure in DD stratification nearly always display a thermohaline staircase structure, in which relatively homogeneous mixed layers are separated by sharp high-gradient interfaces. An important - and not entirely understood - question is what determines the enhanced fluxes of  $T$  and  $S$  in these thermohaline staircases. In order to simplify this problem, a number of laboratory studies have been conducted on a single interface with mixed layers on either side (Marmorino and Caldwell, 1976; Linden and Shirtcliffe, 1978; Newell, 1984; Fernando, 1989). Herein we describe a series of fully three-dimensional direct numerical simulations (DNS) of a single DD interface with a similar setup to previous laboratory experiments. The DNS reveal a detailed picture of the DD convection process that compliments and extends our current knowledge.

	Dimensional scales		Dimensionless parameters			
	$\Delta T \times 10^3$ (kg m <sup>-3</sup> )	$h_T$ (cm)	$Ra_I \times 10^{-4}$	$R_\rho$	Pr	$\tau$
Simulations	0.4 - 1.2	5 - 13	1.1 - 6.7	2 - 6	6.25	0.035
Lake Kivu	1.7	8.8	8.5	2 - 6	$\approx 6.25$	$\approx 0.01$

Table 1: The range of parameters and scales in the simulation, and the median of those measured in the thermohaline staircase of Lake Kivu by Sommer et al. (2011).

## 2 Methods

The DNS are performed with the model previously described by Winters et al. (2004), which has been extended by Smyth et al. (2005) to include a second scalar ( $S$ ) that is resolved on a grid that is twice as dense as the other fields. It is therefore specially suited to study flows with small  $S$  diffusivities.

The simulations are performed in a rectangular domain with dimensions of  $\{L_x, L_y, L_z\} = \{33, 33, 66\}$  cm, with  $z$  denoting the vertical direction and  $x, y$  the horizontal directions. The boundary conditions are periodic in the horizontal and no-flux in the vertical for  $T$ ,  $S$ , and momentum. These boundary conditions resemble the ‘run-down’ experiments of Shirtcliffe (1973) and Newell (1984) in that the DD instability extracts energy from a finite reservoir of potential energy present in the gravitationally unstable  $T$ -field.

The simulations are initiated with profiles of  $T$  and  $S$  that have the same initial interface thicknesses (5 cm), and density jumps across them of  $\Delta T = 0.0012$  kg m<sup>-3</sup> and  $\Delta S = 2\Delta T$ . These scales are motivated by recent measurements within the thermohaline staircase of Lake Kivu (East Africa) by Schmid et al. (2010) and Sommer et al. (2011). Given these scales, as well as the kinematic viscosity  $\nu$ , an average reference density  $\rho_0$ , and the molecular scalar diffusivities of  $\kappa_T$  and  $\kappa_S$ , it is possible to define the following dimensionless parameters

$$Ra_I \equiv \frac{g\Delta T h_T^3}{\rho_0 \nu \kappa_T}, \quad R_\rho \equiv \frac{\Delta S}{\Delta T}, \quad Pr \equiv \frac{\nu}{\kappa_T}, \quad \tau \equiv \frac{\kappa_S}{\kappa_T}, \quad \text{and} \quad r \equiv \frac{h_T}{h_S}. \quad (1)$$

These correspond to the interfacial Rayleigh number, density ratio, Prandtl number, Lewis number, and interfacial thickness ratio. Here the interface thickness of the  $T$  and  $S$  profiles are defined by the relation

$$h_\theta \equiv \Delta\theta / \left( \frac{d\theta}{dz} \right)_{\theta_0}, \quad (2)$$

where  $\theta$  represents  $T$  and  $S$ , and  $\theta_0$  denotes the isoscalar surface that defines the mid-point of the interface.

It is now possible to compare the dimensionless numbers from the simulation with the typical range that is present in Lake Kivu. This is done in Table 1. Although a number of simulations have been performed at different domain sizes and  $\tau$ , for brevity we describe here only a single simulation at  $\tau = 0.035$ . This value is close to the heat-salt value of  $\tau = 0.01$  that is present in the oceans and Lake Kivu, and was chosen based on the availability of computational resources.

In addition, random noise is applied to the velocity field about the interface level at the

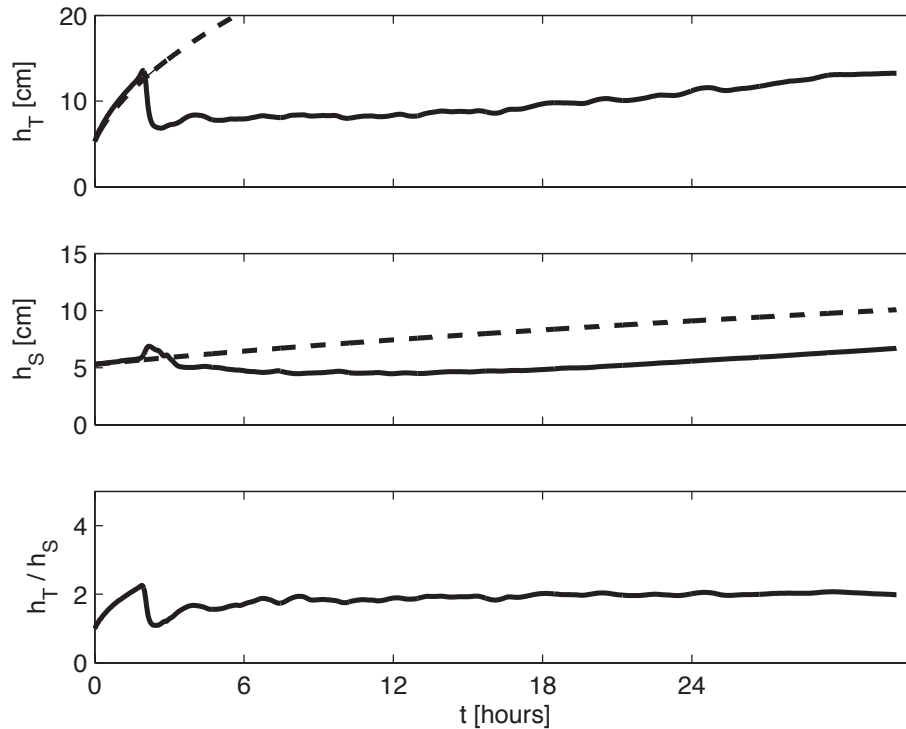


Figure 1: Evolution in time of the average interface thicknesses  $h_T$  and  $h_S$ . The ratio  $r = h_T/h_S$  is also plotted, and shows little variation about the value of  $r = 2$ . Interface growth by purely molecular diffusion is given by the dashed curves.

initial time step in order to seed the growth of instabilities that form in the vicinity of the interface.

### 3 Time evolution

With an initial condition of equal interface thicknesses ( $r = 1$ ) and  $R_\rho = 2$ , the  $TS$ -field is initially in a stable state. This was recently shown to be the case by the stability analysis of a diffusive interface by Carpenter et al. (2011) for  $\tau = 0.01$ , which is close to  $\tau = 0.035$  for no significant differences. However, as the interfaces thicken in time through molecular diffusion, a larger  $h_T$  will develop due to the larger  $T$  diffusivity, and so  $r$  increases. This has the effect of producing gravitationally unstable boundary layers on each side of the interface, since  $T$  is in a gravitationally unstable configuration. The evolution in time of the average interface thicknesses and their ratio is shown in figure 1. The initial phase of growth is by pure molecular diffusion until the time  $t = 2$  hours. The growth of the interfaces in time assuming only molecular diffusion is acting is plotted in figure 1(a,b) with the dashed line. It can be seen that after  $t = 2$  hours, a different process is acting to change the interface thicknesses. At  $t = 2$  hours the unstable boundary layers (with an  $r = 2$ ) break away, creating a turbulent flow in the mixed layers, and sharpening the interfaces. The subsequent decrease of  $h_S$  until approximately  $t = 15$  hours appears to be a transient period where the interfaces are adjusting to the preferred  $r = 2$  state. This  $r = 2$  state is then maintained throughout the rest of the simulation while many other parameters are ‘running down’ in time (e.g.,  $h_T$ ,  $R_\rho$ ,  $Ra_I$ ). This value is also in close agreement with the observations made in Lake Kivu by Sommer et al. (2011, see also this conference proceedings).

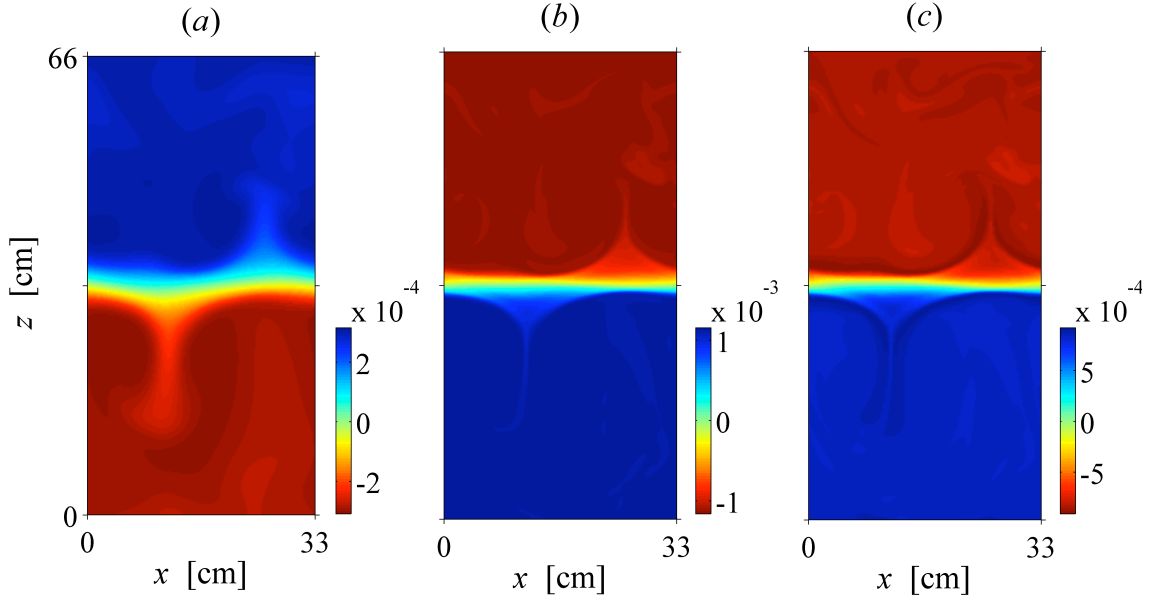


Figure 2: Two-dimensional slices of the (a)  $T$ , (b)  $S$ , and (c)  $\rho - \rho_0$  fields.

#### 4 Interface structure

The results presented in the previous section show that there is a so-called ‘double boundary layer’ structure present at the interface, meaning that the  $T$  interface is thicker than the  $S$  interface, producing gravitationally unstable boundary layers. This has been observed by previous investigators (Marmorino and Caldwell, 1976; Fernando, 1989), but never in a quantitative manner. It can also be seen directly from the two-dimensional slices of the  $T$ ,  $S$ , and  $\rho - \rho_0$  fields shown in figure 2.

It is immediately apparent from the  $T$  and  $S$  fields plotted in figure 2(a,b) that the smaller diffusivity of  $S$  relative to that of  $T$  produces much finer scales with sharper features. This mismatch between the  $T$  and  $S$  fields is responsible for producing buoyancy anomalies in the diffusive boundary layer at the edges of the interface, as well as in localized regions within the mixed layers. The flow structure within the mixed layers appears in the form of convection cells – usually with only one or two cells within the domain. These cells are fed by plumes that form on the edges of the interface, and two such plumes (one in the upper and lower mixed layers) can be seen in figure 2.

#### 5 Fluxes

Of central importance in the study of double diffusive interfaces is the  $T$ -flux  $F_T$ , in  $[\text{kg m}^{-2} \text{s}^{-1}]$ , through the interface. Enhanced fluxes occur due to the sharp high-gradient interface being maintained against the effects of molecular diffusion, which tend to broaden the interface (see figure 1). It has become customary to normalize  $F_T$  by the standard “4/3 flux law” that is used in the case of single component convection through a solid

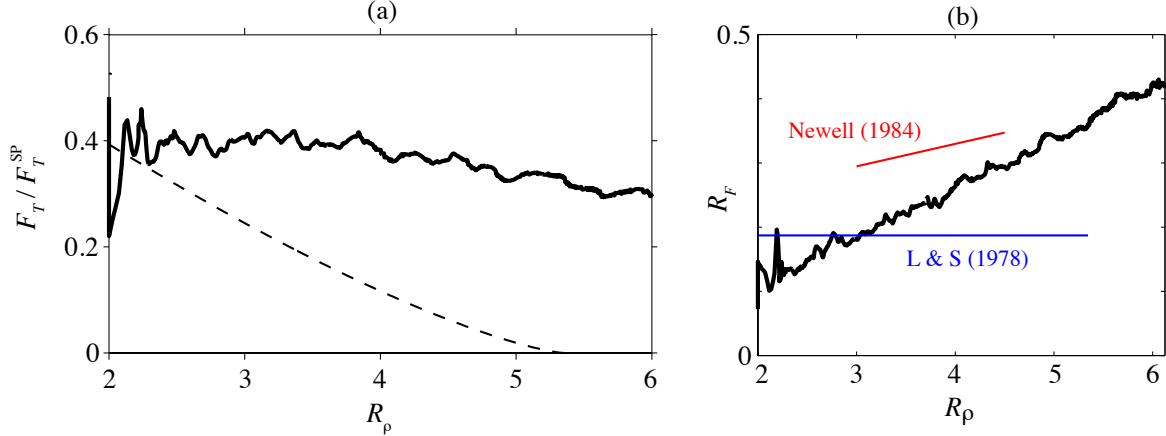


Figure 3: (a) The  $T$ -flux through the interface plotted against  $R_\rho$ , which is changing in time. The  $T$ -flux has been normalized by that predicted by a simple scaling theory of a solid plane (SP) boundary  $F_T^{\text{SP}}$ . (b) The flux ratio  $R_F = F_S/F_T$  against  $R_\rho$ . Plotted in (a,b) is the prediction of Linden and Shirtcliffe (1978) (dashed line in a, and blue line in b), which is only applicable for  $R_\rho < \tau^{-1/2}$ , with  $\tau^{-1/2} = 5.3$  in this case. The prediction of Newell (1984) is shown by the slope of the red line in (b).

plane boundary, which is given by

$$F_T^{\text{SP}} = \lambda^{\text{SP}} \kappa_T \left( \frac{g}{\rho_0 \nu \kappa_T} \right)^{1/3} (\Delta T)^{4/3}. \quad (3)$$

Here,  $\lambda^{\text{SP}}$  is a coefficient usually taken as 0.085. The surface through which the total temperature flux  $F_T$  is calculated, is taken as the iso-temperature surface corresponding to the central interface level, i.e.,  $T_0 = \Delta T/2$ . Using the framework of Winters and D'Asaro (1996), we define the coordinate  $z_b$  such that  $T(z_b)$  gives the resorted 'background' temperature profile, found by rearranging each grid point in the three-dimensional domain into a single monotonic profile. The total temperature flux through the iso-temperature surface  $T_0$  is then computed by

$$F_T = \frac{d}{dt} \int_0^{z_b(T_0)} T(z_b, t) dz_b, \quad (4)$$

corresponding to the total change in heat content in the domain above  $T_0$ .

The  $T$ -flux, scaled with  $F_T^{\text{SP}}$ , for the simulation is shown in figure 3, along with the prediction of Linden and Shirtcliffe (1978). It shows that the  $T$ -flux is approximately 40% of that which would occur if the interface was replaced by a perfectly conducting solid plane boundary with the same  $\Delta T$  between the boundary and the ambient fluid. Since  $R_\rho$  is increasing approximately linearly with time, the  $R_\rho$ -axis can be considered a scaled time axis. Although there is agreement with the 4/3 flux law for the initial times (i.e., when  $R_\rho$  is approximately less than 4) there does appear to be a dependence on  $R_\rho$ , as is predicted by many previous theories and experiments (e.g., Linden and Shirtcliffe, 1978; Fernando, 1989; Kelley, 1990). This can be seen in the departure of the curve in figure 3 with the horizontal.

The  $S$ -flux that accompanies  $F_T$  may be seen by considering the flux ratio, defined as  $R_F \equiv F_S/F_T$ , and plotted as a function of  $R_\rho$  in figure 3(b). A linear increase of  $R_F$  with  $R_\rho$  can clearly be seen. This was predicted by Newell (1984) for intermediate and

large  $R_\rho \gtrsim \tau^{-1/2} = 5.3$ , and is in reasonable agreement with the simulation. This result is in contrast to the observations of Turner (1965) and the theory of Linden and Shirtcliffe (1978) predicting an  $R_F$  that is constant over a range of  $R_\rho$ , and illustrates the transient nature of the diffusive interface as described by Newell (1984).

## 6 Conclusions

The direct numerical simulation described here has allowed for an in depth look at the diffusive interface. It is designed to reproduce the conditions present in the thermohaline staircase of Lake Kivu, as well as the setup of previous laboratory experiments. It has revealed a ‘double boundary layer’ structure, in which the  $T$  interface is generally thicker than the  $S$  interface by a factor of two. This gravitationally unstable boundary layer generates convective plumes that create turbulence and a large-scale circulation in the mixed layers. The  $T$ -flux generated through the interface cannot be fully described by the ‘4/3 flux law’, and is likely time, or  $R_\rho$ , dependent. The coupled fluxes of  $T$  and  $S$  are found to agree reasonably well with the transient prediction of Newell (1984) over the entire duration of the simulation.

## References

- Carpenter, J., Sommer, T., and Wüest, A. (2011). Stability of a double-diffusive interface in the diffusive regime. *J. Phys. Oceanogr.*, (submitted).
- Fernando, H. (1989). Buoyancy transfer across a diffusive interface. *J. Fluid Mech.*, 209:1–34.
- Kelley, D. (1990). Fluxes through diffusive staircases: a new formulation. *J. Geophys. Res.*, 95:3365–3371.
- Kelley, D., Fernando, H., Gargett, A., Tanny, J., and Ozsoy, E. (2003). The diffusive regime of double-diffusive convection. *Prog. Oceanogr.*, 56:461–481.
- Linden, P. and Shirtcliffe, T. (1978). The diffusive interface in double-diffusive convection. *J. Fluid Mech.*, 87:417–432.
- Marmorino, G. and Caldwell, D. (1976). Heat and salt transport through a diffusive thermohaline interface. *Deep-Sea Res.*, 23:59–67.
- Newell, T. (1984). Characteristics of a double-diffusive interface at high density stability ratios. *J. Fluid Mech.*, 149:385–401.
- Schmid, M., Busbridge, M., and Wüest, A. (2010). Double-diffusive convection in Lake Kivu. *Limnol. Oceanogr.*, 55(1):225–238.
- Shirtcliffe, T. (1973). Transport and profile measurements of the diffusive interface in double diffusive convection with similar diffusivities. *J. Fluid Mech.*, 57:27–43.
- Smyth, W., Nash, J., and Moum, J. (2005). Differential diffusion in breaking Kelvin-Helmholtz billows. *J. Phys. Oceanogr.*, 35:1004–1022.
- Sommer, T., Carpenter, J., Schurter, M., Lueck, R., Schmid, M., and Wüest, A. (2011). Temperature and salinity microstructure of a double-diffusive staircase. (in prep.).

- Turner, J. S. (1965). The coupled turbulent transports of salt and heat across a sharp density interface. *Int. J. Heat Mass Transfer*, 8:759–767.
- Winters, K. and D’Asaro, E. (1996). Diascalar flux and the rate of fluid mixing. *J. Fluid Mech.*, 317:179–193.
- Winters, K., MacKinnon, J., and Mills, B. (2004). A spectral model for process studies of rotating, density-stratified flows. *J. Atmos. Ocean. Tech.*, 21:69–94.
- You, Y. (2002). A global ocean climatological atlas of the Turner angle: implications for double-diffusion and water-mass structure. *Deep-Sea Res.*, 49:2075–2093.